A Conformational Change Associated with the Phototransformation of *Pisum* Phytochrome A As Probed by Fluorescence Quenching†

Todd A. Wells,‡ Miki Nakazawa,§ Katsushi Manabe,*,§ and Pill-Soon Song*,‡

Department of Chemistry and Institute for Cellular and Molecular Photobiology, University of Nebraska, Lincoln, Nebraska 68588-0304, and Department of Biology, Yokohama City University, Seto 22-2, Kanazawa-ku, Yokohama 236, Japan

Received August 16, 1993; Revised Manuscript Received November 10, 1993®

ABSTRACT: Dynamic quenching of the two lifetime component tryptophan fluorescence of *Pisum* phytochrome has revealed differential accessibility of certain residues. Both acrylamide and Tl^+ ions showed preferential exposure of some tryptophans in Pfr-phytochrome. Greater k_q's for Pfr are, however, in contrast with values for *Avena* phytochrome in which Pr → Pfr conversion impedes Tl^+ access. The Pr short lifetime component was more accessible to Cs^+; however, the long component accessibility was approximately 2-fold higher in Pfr. 2-Hydroxy-5-nitrobenzyl bromide (HNB-Br) modification of native *Pisum* phytochrome was used to reduce the total number of fluorescent tryptophans. The absence of the fluorescence contributions of the three residues which reacted with HNB-Br in both photoisomers increased the Tl^+ K_{sv}'s for Pr and Pfr. The two additional HNB-Br modifications specific for Pfr resulted in a reversal of the Stern–Volmer plots relative to the unmodified protein. The regions around four of the 10 tryptophans may represent conformationally photoresponsive areas in *Pisum* phytochrome A. Furthermore, topographic changes associated with the phytochrome phototransformation are not confined to the 58-kDa chromphore domain, and they involve most if not all of the region from Trp-365 to Trp-787. We also provide evidence that the protein conformation in this region is not completely conserved between *Pisum* and *Avena* phytochromes.

Phytochrome, a tetrapyrrolic chromoprotein, mediates a number of red light induced morphogenic and developmental responses in plants. The monomeric molecular mass of type A phytochrome ranges from 120 to 125 kDa, depending on the species (Vierstra et al., 1984). It exists in two interconvertible photoisomers, the red light absorbing Pr[1] (Q_y absorption at 666 nm) and the physiologically active Pfr (far-red Q_y absorption peak at 730 nm). Upon photoconversion (Pr → Pfr) the chromphore undergoes a *Z* to *E* isomerization about the C-15=C-16 double bond [for a recent review, see Furuya and Song (1994)]. Isomerization induces secondary structure alterations as well as topographic rearrangement. These unique structural features of Pfr are important because of their possible functional role in light signal transduction.

Changes in the protein secondary structure seem to be confined to the N-terminal region, where a photoreversible increase in α-helix content, involving the 6-kDa amino-terminal residue, occurs upon conversion to Pfr (Sommer & Song, 1990; Park et al., 1992). Evidence of topographic changes accompanying Pr to Pfr phototransformation has also been found. Limited proteolysis (for example, Vierstra & Quail, 1983; Lagarias & Mercurio, 1985; Grimm et al., 1988; Nakazawa et al., 1993), phosphorylation (McMichael & Lagarias, 1989), and antibody epitope recognition (Cordonnier et al., 1985; Schenider-Poetsch et al., 1989) have produced evidence for sites of increased exposure in Pfr-phytochrome. Phototransformation also results in a net increase in the hydrophobic surface of the protein (Tokutomi et al., 1981; Hahn et al., 1984; Nakazawa et al., 1991). These macroscopic rearrangements are consistent for both *Pisum* and *Avena* phytochrome A. Phytochrome A contains 10 Trp residues (Vierstra et al., 1984; Hershey et al., 1985). These tryptophans span the central region of the protein, or domains C–F of the model proposed by Romanowski and Song (1992). Although complicated by the number of Trp residues, dynamic quenching studies used on *Avena* phytochrome showed there are substantial alterations in the molecular and electrostatic microenvironments of the fluorescent tryptophans (Singh et al., 1988). Singh and Song (1990) resolved the fluorescence decays of these indole-containing residues into two lifetime components. Quenching behavior demonstrated each component, short and long, represented a separate group of Trp residues which are differentially exposed in Pr and Pfr.

Cationic Cs^+ and Tl^+, anionic I^-, and neutral acrylamide were used to identify topographic differences in *Pisum* Pr and Pfr. Anionic and cationic quenchers can provide information on the electrostatic environment of Trp residues (Eftink, 1991). The neutral but polar quencher acrylamide was used to sample those tryptophans that are inaccessible to ionic quenchers (Eftink, 1991).

In order to reduce the number of fluorescent tryptophans we have used 2-hydroxy-5-nitrobenzyl bromide. HNB-Br reacts with Trp residues in proteins under mild conditions, pH 4–8 (Horton & Koshland, 1967). The modified tryptophans are nonfluorescent (Naik & Horton, 1973) and can be readily quantified (Horton & Koshland, 1967). Nakazawa and Manabe (1993) have shown that Pfr contains a larger number of reactive Trp residues than does Pr.

† This work was supported by National Institutes of Health Grant GM-36956.

* To whom correspondence should be addressed.

‡ University of Nebraska, Lincoln.

§ Yokohama City University.

® Abstract published in *Advance ACS Abstracts*, January 1, 1994.

[1] Abbreviations: Pr, red absorbing form of phytochrome; Pfr, far-red absorbing form of phytochrome; HNB-Br, 2-hydroxy-5-nitrobenzyl bromide; SAR, specific absorbance ratio; fwhm, full width at half-maximum; EDTA, ethylenediaminetetraacetic acid; Pr_{Pr}, Pr_{Pfr}, Pfr_{Pr}, and Pfr_{Pfr}, the photoisomer in which the HNB-Br modification was performed is given as the normal case, Pr or Pfr, and the form in which quenching was done is represented by the subscript Pr or Pfr.

0006-2960/94/0433-708$04.50/0

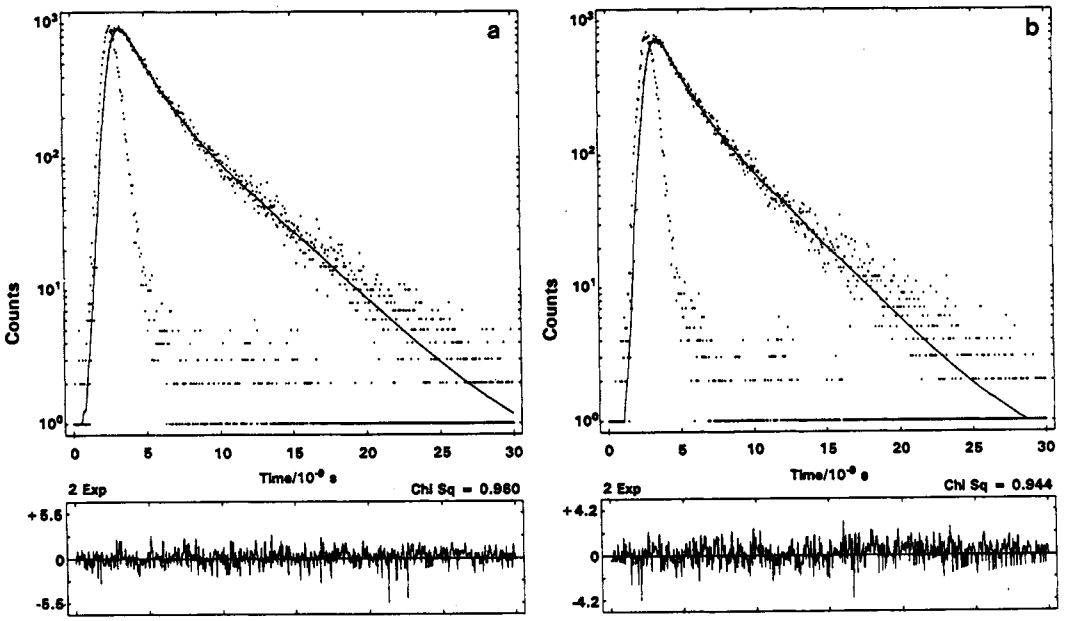

FIGURE 1: Time-resolved decays of the intrinsic tryptophan fluorescence for both (a) Pr, *Pisum* type A phytochrome, and (b) Pr + 16 mM Tl^+. The excitation and emission monochromators were set at 292 and 360 nm, respectively, and a sample temperature of 277 K was maintained throughout.

Pisum phytochrome Stern–Volmer quenching data is incongruous with that obtained for *Avena* phytochrome and represents biophysical evidence for conformational variability between the *Avena* and the *Pisum* chromoproteins. These differences in combination with the differences in the primary structure of these two species of phytochrome have also allowed for localization of the conformational changes resulting from Pr to Pfr phototransformation.

MATERIALS AND METHODS

Phytochrome. Pisum phytochrome A (121 kDa) from 6-day-old etiolated pea seedlings was prepared by the method of Nakazawa et al. (1991), with a specific absorbance ratio (SAR = A_{666}/A_{280}) in the range of 0.9–1.02. Reactions with 2-hydroxy-5-nitrobenzyl bromide (HNB-Br) were done by the procedure of Nakazawa and Manabe (1993). *Avena* phytochrome was prepared by a modification of the Vierstra and Quail (1983) and Chai et al. (1987) methods as described in Sommer and Song (1990).

Time-Resolved Fluorescence Measurements. All tryptophan fluorescence decay curves were obtained by time-correlated single photon counting (O'Connor & Phillips, 1984). Dynamic quenching data were obtained using an Edinburgh 299T fluorescence decay time spectrometer, equipped with a nanosecond spark source. Monochromators, based on the EI-121 series, facilitated selection of both excitation (292 nm) and emission (360 nm) wavelengths. The instrument profiles were determined by scattering the 292-nm excitation pulse through Ludox HS-30 colloidal silica (duPont). A full-width half-maximum (fwhm) of 1.0 ± 0.1 ns was maintained for all measurements. Reconvolution of fluorescence decays was performed using the Edinburgh FLA-900 fluorescence lifetime analysis package.

Samples were cooled to 4 °C by a circulating water bath. No significant photoconversion of either form of the phytochrome resulted from the 292-nm excitation source (a H_2-filled nanosecond flash lamp). A Cole-Palmer microscopic illuminator (supplied with a 660-nm interference filter from The Optometrics Corp.) and the 4 °C temperature were used to counteract dark reversion from the Pfr form to the Pr form (Partis & Thomas, 1991). Thirty-second pulses every 5 min were used to maintain an equilibrium shifted to the Pfr form for measurements of native pea phytochrome. HNB-Br-modified phytochrome exhibits faster dark reversion and required 15-s pulses every 1 min to maintain a similar photoequilibrium. Light pulse duration and repetition rate were controlled via a solid-state relay interfaced with a 386-33-MHz PC. Photobleaching was limited by a combination of the above pulsing and attenuation of the light intensity to below 9.08 $\mu W/cm^2$ with an AC power modulator.

Picosecond fluorescence decay measurements were made using a time-correlated single photon counting instrument with enhanced time resolution as described in Chen et al. (1993). An excitation wavelength of 300 nm was used. Emission wavelengths were selected using a series of 320- and 345-nm cutoff filters. The instrument profile was 50–70 ps (fwhm), giving a 5–7-ps time resolution upon deconvolution. Sample handling was similar to that discussed above.

Stern–Volmer Quenching. Stock solutions of quenchers, 5 M thallium acetate, 5 M CsCl, 8 M acrylamide, and 5 M KI, were each prepared using 10 mM potassium phosphate buffer containing 1 mM EDTA and 14 mM 2-mercaptoethanol. Aliquots of these stock solutions were added separately to 250-μL samples of 0.15 A_{280} phytochrome (native and HNB-Br-modified). Quenching data were plotted in the standard Stern–Volmer manner. The Stern–Volmer quenching constant, K_{sv}, and the quenching rate constant, k_q, were determined as follows:

$$\tau_0/\tau = 1 + K_{sv}[Q] = 1 + k_q\tau_0[Q]$$

where τ_0 and τ are the lifetimes in the absence and presence of quencher, respectively.

RESULTS

Time-Resolved Fluorescence Measurements. The fluorescence decays for the Pr and Pfr forms of both *Pisum* and *Avena* phytochromes were analyzed by reconvolution fit. The Marquardt search algorithm yielded reliable fits when limited to just two exponentials. Representative Trp fluorescence decays are shown in Figure 1. The statistical effectiveness of

Table 1: Trp Fluorescence Decay Parameters of the Two Lifetime Components[a]

fluorophore	τ_1 (ns)	a_1[b]	τ_2 (ns)	a_2[b]
Pr	1.38 ± 0.06	0.42	4.08 ± 0.05	0.58
Pfr	1.32 ± 0.05	0.38	4.96 ± 0.05	0.61
Pr_{Pr}	1.05 ± 0.07	0.30	4.17 ± 0.09	0.70
Pr_{Pfr}	1.16 ± 0.07	0.31	4.56 ± 0.09	0.69
Pfr_{Pr}	0.74 ± 0.04	0.36	3.70 ± 0.07	0.64
Pfr_{Pfr}	0.64 ± 0.03	0.42	4.18 ± 0.08	0.58

[a] Fluorescence lifetime measurements were carried out at 297 K with an excitation wavelength of 292 nm and an emission wavelength of 360 nm. [b] a is the relative amplitudes of each component. Standard deviations less than 0.001 were obtained for all amplitudes.

limiting the nonlinear least-squares analysis of a multitryptophan protein to only two exponentials is illustrated by both the χ^2 values and the plotted residuals. No χ^2 fell outside of the range of 0.8–1.2 and all residuals were randomly distributed with respect to time as in Figure 1. Fitting of the fluorescence decays yielded lifetimes of 1.38 and 4.08 ns for Pr and 1.32 and 4.96 ns for Pfr. The longer component shows the greatest relative amplitude (see Table 1).

Stern–Volmer Quenching of Pea Phytochrome. The short and long lifetime components of the decays were subjected to Stern–Volmer analysis individually. Quenching rate constants in the range of those for acrylamide (Table 2) are indicative of tryptophans which are significantly exposed. Proteins with exposed Trp residues and little secondary structure generally have k_q values near 4×10^9 M^{-1} s^{-1} (Eftink, 1991). Stern–Volmer constants and bimolecular rate constants for the short component differ little between the red and far-red absorbing forms of phytochrome. However, k_q's of 1.9×10^9 M^{-1} s^{-1} and 1.4×10^9 M^{-1} s^{-1} for Pfr and Pr long components, respectively, demonstrate that these residues are more accessible in Pfr.

When shielding by the protein matrix is steric in nature, similar results are usually obtained for acrylamide and iodide (Eftink, 1991). Iodide concentration in the range of 100–400 mM produced Stern–Volmer constants less then 1 M^{-1} for all except the short component of the Pr form. Red light induced conformational changes in the chromoprotein decrease the k_q for the short component of the intrinsic Trp fluorescence from 1.6×10^9 M^{-1} s^{-1} (Pr) to 5.2×10^8 M^{-1} s^{-1} (Pfr), thus lowering the net collision cross section of the affected residues. On the other hand, the net collision cross section of the long component remains relatively constant irrespective of the photoisomer studied (Table 2). The elevated Stern-Volmer constant of this lifetime group stems from an increase in the long component decay time on Pr → Pfr photoconversion (Tables 1 and 2).

The cationic quencher Cs^+ was able to probe both the electrostatic and steric shielding of the Trp residues which contribute to the short and long components. Like I^-, differential exposure to Cs^+ was not easily observable by steady-state techniques, but the time-resolved measurements summarized in Table 2 show that Cs^+ was best able to access the tryptophans of the Pr short component (opposite of acrylamide). The long component residues in close proximity with increasing concentrations of Cs^+ illustrate behavior analogous with acrylamide, showing relative increases in surface exposure upon conversion to Pfr (i.e., 1.3×10^9 M^{-1} s^{-1} and 1.9×10^9 M^{-1} s^{-1} for Pr and Pfr, respectively).

The second cationic quencher, Tl^+, was employed for two reasons. One, the relative quenching efficiency of Tl^+ is 1.0 as compared to a value of 0.2 for Cs^+. Two, Tl^+, 1.47 Å, has a smaller ionic radius than Cs^+, 1.67 Å, and is able to penetrate farther into the protein matrix. Short component residues are readily accessible to this cationic quencher, even more so than for Cs^+. The unusually large k_q values for this component, 1.0×10^{10} M^{-1} s^{-1} and 2.4×10^{10} M^{-1} s^{-1} for Pr and Pfr, respectively, indicate the presence of amino acid side chains which would cause the accumulation of this quencher in the vicinity of the Trp residues. Note the qualitative reversal of the quenching rate constants with respect to cesium (Table 2). No significant difference was observed between the ability of Tl^+ and Cs^+ to probe the collision cross sections of the Pr long component Trp residues. On the other hand, the magnitude of the K_{sv} and k_q values for Tl^+ quenching of the Pfr long component were greater than those observed for Cs^+.

HNB-Br-Modified Phytochrome. Reaction of HNB-Br and phytochrome (Pr or Pfr) resulted in modified chromoprotein which retained spectral integrity and photoreversibility (Nakazawa & Manabe, 1993). The number of Trp residues modified is three and five for Pr and Pfr, respectively (Nakazawa & Manabe, 1993). Each modified form was analyzed in both the Pr and Pfr photoisomers. Table 1 gives both lifetimes and relative amplitudes for the modified phytochromes. Changes in both short and long component lifetimes are shown.

The ability of Tl^+ to reach and quench tryptophans of both fluorescence lifetime components led to its application on HNB-Br-modified phytochrome. The intent here was to block the fluorescence of exposed trpytophans with the HNB group and then attempt to quench the fluorescence of the remaining residues. Stern-Volmer plots for Tl^+ quenching of phytochrome modified in the red absorbing form (Pr_{Pr} and Pr_{Pfr}) resemble those of the unmodified protein (see Figure 2). However, as can be seen in Table 3, the slopes are much greater for the HNB-modified phytochrome. The removal of the fluorescence contribution of the two Trp residues which react only in the Pfr form in addition to the three modified in Pr dramatically changes the quenching behavior. The tetrapyrrolic chromoprotein now contained half the number of possible fluorescent Trp residues. The result was that the Pr (Pfr_{Pr}) short and long components had the greatest collisional rate constants for Tl^+ quenching (Figure 2 and Table 3).

Table 2: Stern–Volmer and Collisional Rate Constants for *Pisum* Phytochrome Trp Fluorescence Quenching[a]

	short component (τ_1)				long component (τ_2)			
	Pr		Pfr		Pr		Pfr	
quencher	K_{sv}	k_q	K_{sv}	k_q	K_{sv}	k_q	K_{sv}	k_q
Tl^+	14.0 ± 1.9	10.1 ± 1.5	39.6 ± 3.8	30.0 ± 3.1	5.4 ± 0.4	1.3 ± 0.1	26.0 ± 2.0	5.2 ± 0.4
Cs^+	8.8 ± 0.6	6.4 ± 0.5	6.1 ± 0.5	4.6 ± 0.2	5.2 ± 0.5	1.3 ± 0.1	9.4 ± 0.9	1.9 ± 0.2
I^-	1.9 ± 0.2	1.4 ± 0.1	0.6 ± 0.1	0.5 ± 0.0[b]	0.8 ± 0.0[b]	0.2 ± 0.0[b]	0.9 ± 0.2	0.2 ± 0.0[b]
acrylamide	3.9 ± 0.3	2.8 ± 0.2	4.3 ± 0.4	3.2 ± 0.3	5.9 ± 0.5	1.5 ± 0.1	9.6 ± 0.9	1.9 ± 0.2

[a] Units are expressed in M^{-1} for K_{sv} and $\times 10^9$ M^{-1} s^{-1} for k_q. [b] Standard error is less than 0.05.

Table 3: Stern–Volmer and Collisional Rate Constants for Tl^+ Quenching of HNB-Br-Modified *Pisum* Phytochrome Trp Fluorescence[a]

	Pr_{Pr}		Pr_{Pfr}		Pfr_{Pr}		Pfr_{Pfr}	
component	K_{sv}	k_q	K_{sv}	k_q	K_{sv}	k_q	K_{sv}	k_q
short (τ_1)	75.1 ± 11	71.5 ± 11	100 ± 7.3	86.5 ± 8.0	58.0 ± 1.9	78.4 ± 5.1	11.9 ± 1.7	18.6 ± 2.7
long (τ_2)	17.6 ± 3.9	4.2 ± 0.9	35.8 ± 2.2	7.8 ± 0.5	13.9 ± 1.0	3.7 ± 0.3	9.1 ± 1.4	2.2 ± 0.3

[a] Units are expressed in M^{-1} for K_{sv} and $\times 10^9$ M^{-1} s^{-1} for k_q.

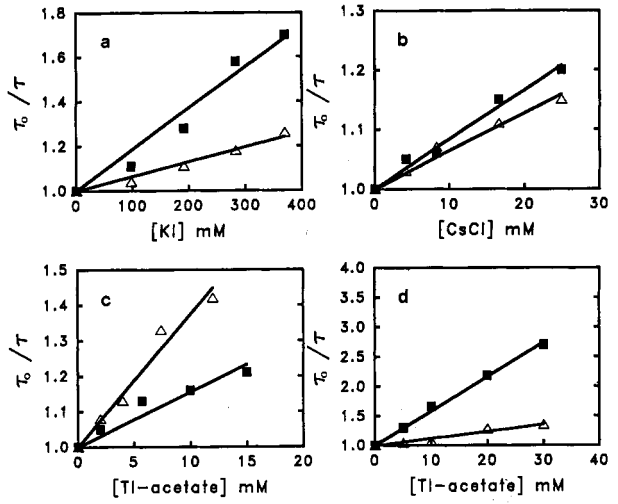

FIGURE 2: Stern–Volmer plots for (a) I^-, (b) Cs^+, and (c and d) Tl^+. Panels a–c are quenching of the short lifetime component of native *Pisum* phytochrome. Pr (■); Pfr (△). Panel d is quenching of *Pisum* phytochrome HNB-Br modified in the Pfr form. Only τ_1 is shown. Pfr_{Pr} (■); Pfr_{Pfr} (△). Conditions were the same as in Figure 1.

DISCUSSION

Four component decays in *Avena* phytochrome A were reported by Schaffner et al. (1991) (14–28 ps, 620–650 ps, 2.20 ns, and 5.30 ns). The 14–28-ps component is below the sensitivity of the current instrument due to the flash lamp excitation. However, we were still unable to resolve this component using a photon-counting instrument with picosecond time resolution (Chen et al., 1993). A tens of picosecond lifetime was observed but it could not be separated from an intrinsic instrument component(s). A component in the range of their 650-ps one could be achieved by fitting the current decays to a three-exponential model. However, a two-exponential fit was used because the addition of a hundreds of picosecond component had little effect on the χ^2, the residuals, or the Durbin–Watson parameters.

Schaffner et al. (1991) deduced that the photoisomer- (Pr- or Pfr-) associated differences in the four component lifetimes and in their decay-associated spectra were so subtle that little structural rearrangement occurs in the vicinity of the respective tryptophans upon phototransformation. However, Toyama et al. (1993) indicated that perturbation of the electronic states of the indole rings by H-bonding or π–π interactions diminishes upon photoconversion (Pr → Pfr). They also showed that the environments of some of the Trp residues are more aliphatic in Pfr than in Pr. Similar results were obtained by Mizutani et al. (1993) for intact, large, and small phytochromes (121, 114, and 58 kDa, respectively). They also reported that conformational changes occur chiefly in areas around Trp residues contained in the 58-kDa chromophore domain.

The 10 tryptophans of *Pisum* phytochrome can be divided into two major classes. The short lifetime group of tryptophans, 1.38 ns (Pr) and 1.32 ns (Pfr), may contain residues which contribute, via Förster-type energy transfer, to the sensitized 680-nm tetrapyrrolic chromophore fluorescence emission proposed by Chai et al. (1987) for *Avena* phytochrome. Lifetimes shorter than that of free Trp in aqueous buffer (2.9 ns for Trp in phosphate buffer) may also result from the presence of amino acids such as Cys, Met, and Gln, efficient quenchers of indole fluorescence, in the vicinity of the Trp residues (Ludescher et al., 1985). Trp residues 365, 773, and 777 have neighboring-SH groups from Cys residues, and Met 474 is adjacent to Trp-473. The amide residues, Gln-359 and Gln-466, may quench the fluorescence of tryptophans 365 and 473.

Singh and Song (1990) reported that both the long and the short components of *Avena* Pr are preferentially quenched by Tl^+ (see Figure 2c for comparison). Their results were checked using the current experimental conditions in order to rule out differences caused by technique; none were observed. Thus, the differences must stem from the state of the environment of each Trp residue (this will be discussed later).

Hydrophobicity profiles show Trp-456 (*Pisum*) is in a hydrophobic stretch. The homologous Trp in *Avena* phytochrome is predicted to be in a hydrophilic region. Arg-459 (*Avena*) is adjacent to Trp-458; this residue is a Leu in *Pisum*. Trp-473 in *Pisum* is possibly quenched by Met-474. No intrinsic quencher is present in the vicinity of *Avena* Trp-475. No Pr/Pfr common cleavage site (Grimm et al., 1988) complementary to that seen in *Avena* can be found near *Pisum* Trp-520 and Trp-531. Lys-568 (*Pisum*), adjacent to Trp-567, is a serine in *Avena*. A relatively hydrophilic region surrounds *Avena* Trp-645; this same region in *Pisum* phytochrome is a hydrophobic stretch. Cys-775 may quench the fluorescence of Trp-774 and Trp-778 (*Avena*) but *Pisum* Trp-773 and Trp-777 have two -SH containing neighbors. Lys-788, juxtaposed to Trp-787, is replaced by Asn-789 in *Avena*.

The diversity in hydrophobic character above would result in variation in the packing density in these regions for *Avena* as compared to *Pisum* phytochrome. Therefore, accessibility to quenchers would also be affected. Any divergence in the electrostatic environments of the tryptophans, such as those above, would also change the relative exposure of the indole ring in *Pisum* and *Avena* phytochromes. Another factor which would yield differential quenching behavior is the presence of intrinsic quenchers. Additional Cys and Met residues found in the *Pisum* phytochrome primary structure would alter the relative distribution of Trp residues in the short and long components.

Despite being in a hydrophilic region, Trp-365 does not react with HNB-Br in either Pr or Pfr (Nakazawa & Manabe, 1993). Nakazawa and Manabe (1993) reported that Trp-473, Trp-520, Trp-531, and Trp-567 are candidates for the HNB-reactive residues in the 58-kDa domain (Figure 3), Trp-456, Trp-473, and Trp-567 being the best choices. Limited proteolysis has revealed that tryptophans near Ala-616 and Ala-753 (Trp-644, Trp-773, and Trp-777) are in or near solvent-accessible zones. Portions of these regions are exposed in both Pr and Pfr (Nakazawa et al., 1993). Two of these Trp residues are modified in Pr and the other is modified in Pfr. Trp-787 was ruled out because it is in the proposed dimerization site of Romanowski and Song (1992). The Trp residues which

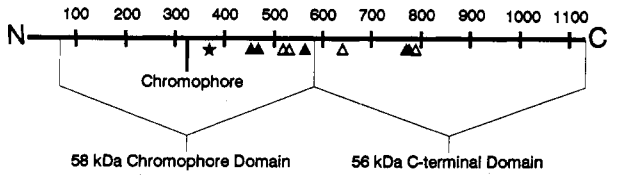

FIGURE 3: Locations of the Trp residues with respect to the amino acid sequence. The Trp residue not modified by HNB-Br in either Pr or Pfr is indicated by a star. Trp residues marked with closed triangles are the most probable sites for HNB-Br modification unique to Pfr. The open triangles represent Trp residues which either are not modified or are modified in both Pr and Pfr.

are modified with the HNB group are also the ones most exposed to the fluorescence quenchers. However, as shown in Figure 2 and Table 3, even after modification of five Trp residues the fluorescence can still be quenched.

It is clear now that topographic changes occur throughout the entire Trp-containing region of the chromoprotein. The differential quenching behavior between pea and oat phytochrome, their primary structure differences, and the HNB-Br modification have led to the conclusion that significant rearrangements are centered around Trp-456, Trp-473, Trp-567, Trp-773, and Trp-777. These residues lie in negatively charged stretches of the amino acid sequence. Exposure to cationic quenchers would be facilitated and topographic changes could enhance the exposure by increasing the number of the negatively charged amino acids in the microenvironments of these tryptophans. A net increase in surface negativity was previously observed by Nakazawa et al. (1991).

Although the tetrapyrrolic chromoproteins have the same function in their respective plants, the microenvironments of the tryptophans are not constant from the monocotyledon *Avena* to the dicotyledon *Pisum*. This variance in microenvironment has led to the differential quenching behavior and has provided evidence that some degree of conformational heterogeneity exists in this region of the protein.

ACKNOWLEDGMENT

We would like to thank Janelle Jones for help in preparing the manuscript. We also thank Dr. Jake Petrich and his group for their assistance in performing the picosecond fluorescence measurements at Iowa State University.

REFERENCES

Chai, Y. G., Singh, B. R., Song, P.-S., Lee, J., & Robinson, G. W. (1987) *Anal. Biochem. 163*, 322–330.

Chen, Y., Rich, R. L., Gai, F., & Petrich, J. W. (1993) *J. Phys. Chem. 97*, 1770–1780.

Cordonnier, M.-M., Greppin, H., & Pratt, L. H. (1985) *Biochemistry 24*, 4246–3253.

Eftink, M. R. (1991) in *Topics in Fluorescence Spectroscopy* (Lakowicz, J. R., Ed.), Vol. 2, pp 52–126, Plenum Press, New York.

Furuya, M., & Song, P.-S. (1994) in *Photomorphogenesis in Plants* (Kendrick, R. E., & Kronenberg, G. H. M., Eds.) pp 105–140, Martinus Nijhoff, Dordrecht, The Netherlands.

Grimm, R., Eckerskorn, C., Lottsspeich, F., Zenger, C., & Rüdiger, W. (1988) *Planta 174*, 396–401.

Hahn, T. R., Song, P.-S., Quail, P. H., & Vierstra, R. D. (1984) *Plant Physiol. 74*, 755–758.

Hershey, H. P., Barker, R. F., Idler, K. B., Lissemore, J. L., & Quail, P. H. (1985) *Nucleic Acids Res. 13*, 8543–8559.

Horton, H. R., & Koshland, D. E., Jr. (1967) *Methods Enzymol. 11*, 556–565.

Lagarias, J. C., & Mercurio, F. (1985) *J. Biol. Chem. 260*, 2415–2423.

Ludescher, R. D., Volwerk, J. J., de Had, G. H., & Hudson, B. S. (1985) *Biochemistry 24*, 7240–7249.

McMichael, R. W., Jr. & Lagarias, J. C. (1989) *Biochemistry 29*, 3872–3877.

Mizutani, Y., Tokutomi, S., Kaminaka, S., & Kitagawa, T. (1993) *Biochemistry 32*, 6916–6922.

Naik, V. R., & Horton, H. R. (1973) *J. Biol. Chem. 248*, 6709–6717.

Nakazawa, M., & Manabe, K. (1993) *Plant Cell Physiol. 34*, 1097–1105.

Nakazawa, M., Yoshida, Y., & Manabe, K. (1991) *Plant Cell Physiol. 32*, 1187–1194.

Nakazawa, M., Hayashi, H., Yoshida, Y., & Manabe, K. (1993) *Plant Cell Physiol. 34*, 83–91.

O'Connor, D. V., & Phillips, D. (1984) *Time-correlated Single Photon Counting*, Academic Press, Orlando, FL.

Parker, W., Partis, M., & Song, P.-S. (1992) *Biochemistry 31*, 9413–9420.

Partis, M. D. & Thomas, B. (1991) in *Methods in Plant Biochemistry* (Roger, L. J., Ed.), Vol. 5, pp 233–257, Academic Press, London.

Robbins, D. J., Deibel, M. R., Jr., & Barkely, M. D. (1985) *Biochemistry 24*, 7250–7257.

Romanowski, M., & Song, P.-S. (1992) *J. Protein Chem. 11*, 139–155.

Schaffner, K., Braslavsky, S. E., & Holzwarth, A. R. (1991) in *Frontiers in Supramolecular Organic Chemistry and Photochemistry* (Schneider, H.-J., & Dürr, H., Eds.), pp 421–452, VCH, Weinheim, Germany.

Schneider-Poetsch, H. A. W., Braun, B., & Rüdiger, W. (1989) *Planta 177*, 511–514.

Singh, B. R., & Song, P.-S. (1990) *Planta 181*, 263–267.

Singh, B. R., Chai, Y. G., Song, P.-S., Lee, J., & Robinson, G. W. (1988) *Biochim. Biophys. Acta 936*, 395–405.

Sommer, D., & Song, P.-S. (1990) *Biochemistry 29*, 1943–1948.

Tokutomi, K., Yamamoto, K. T., & Furuya, M. (1981) *FEBS Lett. 134*, 159–169.

Toyama, A., Nakazawa, M., Manabe, K., Takeuchi, H., & Harada, I. (1993) *Photochem. Photobiol. 57*, 391–395.

Vierstra, R. D., & Quail, P. H. (1983) *Biochemistry 22*, 2498–2505.

Vierstra, R. D., Cordonnier, M.-M., Pratt, L. H., & Quail, P. H. (1984) *Planta 160*, 521–528.